INTERNATIONAL ATOMIC ENERGY AGENCY
UNITED NATIONS EDUCATIONAL, SCIENTIFIC AND CULTURAL ORGANIZATION
INTERNATIONAL CENTRE FOR THEORETICAL PHYSICS
I.C.T.P., P.O. BOX 586, 34100 TRIESTE, ITALY, CABLE: CENTRATOM TRIESTE

SMR/534-22

ICTP/WMO WORKSHOP ON EXTRA-TROPICAL AND TROPICAL
LIMITED AREA MODELLING
22 October - 3 November1990

"Advection Schemes: Semi-Lagrangian, Shape Preservation, Positive Definiteness"

Z.I. JANJIC
University of Belgrade
Department of Meteorology
Belgrade, Yugoslavia

Semi-Lagrangian schemes, two aspects:

* [illegible]

* [illegible]

(1) [illegible]

(2) [illegible]

Specific humidity, TKE ...

* Williamson & Rasch 1988, 1989
most organized recent study

* Godunov-type schemes (Priestly, ECMWF 87)
- piecewise constant
- -"- linear
- -"- parabolic

interpolation methods that maintain certain properties suggested by the data. Such properties include monotonicity and convexity, and provide a means of avoiding the oscillations often seen in polynomial interpolation. These methods reduce or eliminate the overshooting possible with the semi-Lagrangian transport method.

We summarize our current work in this report. More details are included in papers being prepared for journal publication. In Section 2 we describe various shape preserving interpolators and summarize an evaluation of their relative performance when applied to several test functions. In Section 3 we show selected examples from applying the interpolators to one-dimensional semi-Lagrangian transport and summarize our more complete study. We consider uniform translation of specified test shapes. In Section 4 we summarize results from the application of the schemes that performed best in the first tests to two-dimensional semi-Lagrangian advection on a plane. The test case is uniform rotation of specified test shapes. We extend the two-dimensional advection on a plane to advection on the surface of the sphere in Section 5 and show that no serious problems are introduced by that geometry. The test case is solid body rotation of test shapes about an axis rotated with respect to the polar axis of the coordinate system. Finally, in Section 6 we compare several methods for calculating the departure point in spherical geometry.

2. *THE INTERPOLATION PROBLEM*

We begin by defining the grid $\{x_i\}_{i=1}^n$, $x_1 < x_2 < \ldots < x_n$, and the data values $\{f_i\}$, $f_i = f(x_i)$. It is also convenient to define the *discrete slopes*

$$\Delta_i = (f_{i+1} - f_i)/(x_{i+1} - x_i) \,. \tag{2.1}$$

The data are locally monotonic at x_i if

$$\Delta_{i-1}\Delta_i > 0 \,, \tag{2.2}$$

and locally convex if

$$\Delta_{i-1} > \Delta_i \,. \tag{2.3}$$

For concave data, the inequality in (2.3) is reversed. We define a piecewise interpolant $p \in C^K[x_1, x_n]$, with $K \geq 0$. On each subinterval $[x_i, x_{i+1}]$, let

$$\theta = (x - x_i)/h_i \,, \qquad h_i = x_{i+1} - x_i \tag{2.4}$$

and

$$p(x) = p_i(\theta) \,. \tag{2.5}$$

The interpolant p is constrained to have the following interpolatory properties

$$p(x_i) = f_i \,, \qquad dp(x_i)/dx = d_i \,. \tag{2.6}$$

Here, d_i is some estimate of the derivative of f at the endpoints of the interval. The interpolant is specified on the subinterval in terms of the data f_i, and the derivative estimates d_i at the endpoints of the subinterval, that is

$$p_i(\theta) = p_i(\theta, f_i, f_{i+1}, d_i, d_{i+1}) \tag{2.7}$$

The interpolant thus adheres to the standard osculatory representation, although the functional form of p_i is not necessarily the usual Hermite cubic polynomial form. In order to reduce the number of schemes involved in the intercomparison, only interpolating forms which involve use of *local* information have been included, i.e., d_i is a function of a few surrounding values of f_i. In this fashion we have excluded from consideration many global schemes; for example, the classic C^2 cubic splines which minimize the integral of the curvature of the interpolant over the entire domain, exponential splines under tension (Spath, 1969), and global versions of the monotone, piecewise interpolants of Fritsch and Carlson (1980) and Delbourgo and Gregory (1983). These schemes require information from the entire domain to interpolate within any one subinterval. Following this restriction, schemes which differ from each other in the following three major ways are considered:

- The method of estimating the derivative is varied according to algorithms that have been suggested in the shape preserving literature.
- The type of interpolating function is varied to encompass cubic polynomials, rational functions, and quadratic Bernstein polynomials with extra knots.
- To guarantee monotonicity or concavity/convexity in the interpolating function, certain constraints are imposed on the derivative estimates. The appropriate constraint depends upon the interpolation form.

It is convenient to address these items in reverse order in the following subsections.

2.1 *Constraints on the derivatives*

Certain constraints must be imposed on the derivative estimates used in the interpolation schemes in order for the interpolants to maintain any convexity/concavity or monotonicity present in the data. The constraints are reviewed in this section, proceeding from the least to the most restrictive form. The constraints can be written in terms of restrictions on the derivative estimates d at the endpoints of an interval, as a function of the discrete slope Δ within the interval. Because of this, the constraint

on d_i based on Δ_{i-1} of the interval to the left may be different from that based on Δ_i of the interval to the right. One may choose to constrain the derivative differently for interpolation over the two intervals in which case the interpolant is C^0, or insist that constraints associated with both intervals be satisfied simultaneously, in which case the interpolant is C^1. When the constraint on d_i depends not only on the discrete slopes over the adjacent intervals Δ_{i-1}, Δ_i, but also the slope estimate d_{i-1}, or d_{i+1} at the other end of the interval, the C^1 interpolants become global. Such forms are not considered in this report.

The requirement that the derivative estimates bound the discrete slope for a C^0 interpolant

$$(d_i - \Delta_i)(\Delta_i - d_{i+1}) > 0 \qquad \text{(NCC0)} \qquad (2.8)$$

and lie between the adjacent discrete slopes for a C^1 interpolant

$$(d_i - \Delta_i)(\Delta_{i+1} - d_i) > 0 \qquad \text{(NCC1)} \qquad (2.9)$$

must be true for the interpolant to remain convex/concave. These requirements are identified as *Necessary Conditions(s) for Convexity/Concavity*, C^0 and C^1, respectively.

In order that the interpolating function be monotonic and C^0 the derivatives must satisfy the *Necessary Condition for Monotonicity*, (NCM0)

$$\begin{aligned} &\text{sign}(d_i) = \text{sign}(\Delta_i) = \text{sign}(d_{i+1}) && \Delta_i \neq 0 \\ &d_i = d_{i+1} = 0 && \Delta_i = 0 \end{aligned} \qquad \text{(NCM0)} \qquad (2.10)$$

that is, the derivative estimate at the end points must have the same sign as the discrete slope on the interval. For a C^1 interpolant

$$\begin{aligned} &\text{sign}(\Delta_{i-1}) = \text{sign}(d_i) = \text{sign}(\Delta_i) && \Delta_{i-1}\Delta_i > 0 \\ &d_i = 0 && \Delta_{i-1}\Delta_i \leq 0\,. \end{aligned} \qquad \text{(NCM1)} \qquad (2.11)$$

The derivative estimate at a data point must have the same sign as the discrete slopes surrounding it or be zero if the data are not monotonic at this point. This condition is the *Necessary Condition for Monotonicity*, C^1 (NCM1).

For the rational and piecewise quadratic interpolation forms to be discussed below, the necessary conditions, NCM0 and NCM1, are also sufficient conditions for monotonicity. Similarly, the NCC0 and NCC1 are sufficient conditions for convexity with these interpolants. On the other hand, for Hermite cubic interpolants NCM0 and NCM1 are necessary but not sufficient for monotonicity and must be augmented by additional constraints on the derivatives.

Fritsch and Carlson (1980) have found both necessary and sufficient conditions for monotonicity of Hermite cubic interpolants. Let $\alpha = d_i/\Delta_i$, $\beta = d_{i+1}/\Delta_i$; then for $\Delta_i \neq 0$ the Hermite cubic interpolant will be monotonic if and only if (α, β) lies within the domain M_{ns} defined by the union of two domains

$$M_{ns} = M_s \cup M_b \qquad (2.12)$$

where

$$M_s(\alpha, \beta) = \{\alpha, \beta : \phi(\alpha, \beta) \leq 0\} \qquad (2.13)$$

$$M_b(\alpha, \beta) = \{\alpha, \beta : 0 \leq \alpha \leq 3, 0 \leq \beta \leq 3\}$$

and

$$\phi(\alpha, \beta) = (\alpha - 1)^2 + (\alpha - 1)(\beta - 1) + (\beta - 1)^2 - 3(\alpha + \beta - 2)\,. \qquad (2.14)$$

If $\Delta_i = 0, d_i = d_{i+1} = 0$ and the necessary condition discussed earlier is also sufficient. Embedded in this domain M_{ns} is the region M_b recognized independently by de Boor and Swartz (1977) which provides a sufficient condition for monotonicity of the Hermite cubic. This sufficient condition

$$0 \leq \alpha \leq 3\,,\ 0 \leq \beta \leq 3 \qquad \text{(SCM)} \qquad (2.15)$$

is easier to apply than the more general necessary and sufficient condition (M_s) in which α and β may be dependent on each other. Throughout the remainder of this report this simpler condition will be referred to as the *Sufficient Condition for Monotonicity* (SCM). As before, we define C^0 and C^1 forms depending on whether the derivatives d are bounded by just Δ of the interval being interpolated or by the Δ of the two adjacent intervals simultaneously.

At an extremum where the data are not monotonic, SCM1 limiting provides a severe restriction as d_i is then zero there. Hyman (1983) has relaxed the SCM1 limiting concept where the data reach a local extremum, and are not monotonic. He proposed the following limit on the derivatives.

$$d_i = \begin{cases} \min\max(0, d_i), 3(0, \Delta_{\min})] & 0 < \Delta_{\min} \\ \max\min(0, d_i), 3(0, \Delta_{\max})] & 0 < \Delta_{\max} \\ 0 & \text{otherwise} \end{cases} \qquad (2.16)$$

$$\Delta_{\min} = \min(\Delta_i, \Delta_{i-1}) \qquad \Delta_{\max} = \max(\Delta_i, \Delta_{i-1}) .$$

This allows for overshoot at local discrete extrema and thus is nonmonotonic but does provide some control of the overshoot and, in particular, prevents oscillations at the edges of flat plateaus.

2.2 *Interpolation forms*

Three types of interpolating functions are considered—all have appeared in the recent literature regarding shape preserving interpolation.

- Cubic polynomials (de Boor and Swartz, 1977; Fritsch and Carlson, 1980; Hyman, 1983; Fritsch and Butland, 1981)
- Rational functions (Gregory and Delbourgo, 1982; Delbourgo and Gregory, 1983, 1985)
- Quadratic Bernstein polynomials with extra knots (McAllister *et al.*, 1977; McAllister and Roulier, 1978, 1981).

The Hermite cubic and rational interpolating funtions can be described using the formalism of Delbourgo and Gregory (1985). Consider the function

$$p_i = P_i(\theta)/Q_i(\theta) \tag{2.17}$$

on the interval $0 \le \theta \le 1$, equivalently $x_i \le x \le x_{i+1}$, where

$$P_i(\theta) = f_{i+1}\theta^3 + (r_i f_{i+1} - h_i d_{i+1})\,\theta^2(1-\theta)$$

and
$$+ (r_i f_i - h_i d_i)\,\theta(1-\theta)^2 + f_i(1-\theta)^3 \tag{2.18}$$

$$Q_i(\theta) = 1 + (r_i - 3)\theta(1-\theta) \tag{2.19}$$

We consider four choices of the parameter r_i

- If $r_i = 3$, p_i reduces to the standard *Hermite cubic* polynomal interpolation form. Recall that the interpolant will be monotonic if the d_i lie within the domain M_b.
- If $r_i = 1 + (d_i + d_{i+1})/\Delta_i$, then P_i and Q_i reduce to quadratic polynomials, and p_i is identified as a *rational quadratic* interpolant. Delbourgo and Gregory (1985) have shown that provided d_i and d_{i+1} satisfy the NCM, p will be monotonic over the subinterval, otherwise this interpolant is not well defined.

- If $r_i = 1 + \max(C_i/c_i, C_i/c_{i+1})$ where $c_i = \Delta_i - d_i$, $c_{i+1} = d_{i+1} - \Delta_i, C_i = d_{i+1} - d_i$, then P_i and Q_i are cubic polynomials and p_i is identified as the *rational cubic interpolant version 1.*
- If $r_i = 1 + c_{i+1}/c_i + c_i/c_{i+1}$, the P_i and Q_i are again cubic polynomials and p_i is identified as the *rational cubic interpolant version 2.* Delbourgo and Gregory (1985) have shown that if the derivatives satisfy the convexity/concavity constraints NCC0 or NCC1 then both rational cubic versions will be concave/convex. If the derivatives satisfy the monotonicity constaints NCM0 or NCM1 then both versions will be monotonic. Delbourgo and Gregory (1985) have also shown that Version 2 is in general more accurate than Version 1.

The piecewise quadratic Bernstein polynomials with extra knots cannot be described using the previous formalism. This interpolant is constructed by piecing together two quadratic Bernstein polynomials within each interval, with the point of intersection (the extra knot) determined by a rather complex algorithm which cannot be succinctly described with a few equations or figures. Because of this, the reader is referred to the descriptions found in the series of original articles (McAllister *et al.*, 1977; McAllister and Roulier, 1978, 1981). The characteristics of the Bernstein polynomials, together with the algorithms developed for constructing the knot, the value of the interpolant at the knot, and the interpolant derivative at the knot guarantee that the interpolant will be monotonic provided NCM is satisfied, and convex/concave provided NCC is satisfied.

2.3 *Derivative estimation procedures*

Table 1 lists the algorithms used in estimating derivatives at the nodes. Several of the algorithms suggested in the literature for shape preserving interpolation which differ for unequally spaced data reduce to a common form when the data become equally spaced. Our first comparison uses equally spaced data, and therefore common algorithms are grouped together. The table also includes an algorithm identified as Cubic, which does not usually appear as a derivative estimate. This scheme arises by computing a cubic interpolant through the four nearest points. The slope at the nearest two points can then be written as a linear combination of the four surrounding data points. Such a scheme results in an interpolant which is only C^0 continuous. It is included because this form of interpolation is often used in semi-Lagrangian problems. The harmonic mean, geometric mean and Fritsch-Butland derivative estimates automatically satisfy the NCM and NCC constraints. The others generally must be modified to satisfy them.

TABLE 1.

Identifier	Algorithm	
Akima (A70, FC80, H83)	$d_i = \begin{cases} \frac{\alpha\Delta_{i-1}+\beta\Delta_i}{\alpha+\beta} \\ \frac{(\Delta_{i-1}+\Delta_i)}{2} \end{cases}$	$\alpha+\beta \neq 0$ $\alpha+\beta = 0$
	$\alpha = \lvert\Delta_{i+1} - \Delta_i\rvert,\ \beta = \lvert\Delta_{i-1} - \Delta_{i-2}\rvert$	
Arithmetic Mean (FC80, GD82, DG83, H83)	$d_i = \frac{(\Delta_{i-1}+\Delta_i)}{2}$	
Deficient Spline		
Geometric Mean (DG83)	$d_i = \begin{cases} \text{sign}(\Delta_i)\sqrt{\Delta_{i-1}\Delta_i} \\ 0 \end{cases}$	$\Delta_{i-1}\Delta_i \geq 0$ $\Delta_{i-1}\Delta_i < 0$
Harmonic Mean (FB84)	$d_i = \begin{cases} \frac{2\Delta_{i-1}\Delta_i}{(\Delta_{i-1}+\Delta_i)} \\ 0 \end{cases}$	$\Delta_{i-1}\Delta_i \geq 0$ $\Delta_{i-1}\Delta_i < 0$
Rational Linear (GD82)		
McAllister-Roulier (MR81)		
Fritsch-Butland (FB84, H83)	$d_i = \begin{cases} \frac{3\lvert\Delta_{i-1}\rvert\lvert\Delta_i\rvert}{\max(\Delta_{i-1},\Delta_i)+2\min(\Delta_{i-1},\Delta_i)} \\ 0 \end{cases}$	$\Delta_{i-1}\Delta_i \geq 0$ $\Delta_{i-1}\Delta_i < 0$
Cubic	$d_i = \begin{cases} \frac{(2\Delta_{i-1}+5\Delta_i-\Delta_{i+1})}{6} \\ \frac{(-\Delta_{i-2}+5\Delta_{i-1}+2\Delta_i)}{6} \end{cases}$	$x \in (x_i, x_{i+1})$ $x \in (x_{i-1}, x_i)$
Hyman (H83)	$d_i = \frac{\Delta_{i-2}-7\Delta_{i-1}+7\Delta_i-\Delta_{i+1}}{12}$	

Algorithms for derivative estimates as they simplify for evenly spaced data. Reference codes are as follows: A70–Akima (1970), DG83–Delbourgo and Gregory (1983), FB84–Fritsch and Butland (1984), FC80–Fritsch and Carlson (1980), GD82–Gregory and Delbourgo (1982), H83–Hyman (1983), MR81–McAllister-Roulier (1981).

2.4 *Intercomparisons of interpolation schemes*

The accuracies of the interpolation schemes have been tested by applying them to three shapes: a Gaussian, a cosine bell, and a triangle. These shapes were chosen because they have similar forms, but may be successively more difficult to approximate accurately. The Gaussian is C^∞, the cosine bell is C^1 and the triangle is C^0. Tests using resolutions of ten points and forty points were performed.

The shapes were successively displaced 100 times, by 1/100 of the grid interval, and measurements of the accuracy were made. This was to establish the sensitivity of the representation to the relative position of the grid and test shape. The accuracy of any one scheme varied by at least a factor of five over the 100 realizations. We intercompared the schemes using the accuracy averaged over all realizations. We have tabulated the error statistics as a function of interpolation form, derivative approximation scheme and derivative limiter in Rasch and Williamson (1987). We included the seven derivative approximations, the five interpolation forms described above and various monotonicity and convexity constraints on the derivatives as appropriate for the interpolation form. We also considered the unconstrained versions for reference.

These tables of errors provide a staggering amount of information and the discussion justifying the conclusion about the interpolation from the tables is somewhat tedious. The tables and discussion are not repeated here. Out of the mass of numbers considered, there are logical inferences to be drawn relating the various schemes to each other. These conclusions may not be universal, as definite known properties of particular fields might be used to advantage in the interpolation scheme. Minor exceptions can be found in our tables that might imply some other scheme is ideal for such specific applications.

We begin by itemizing our conclusions regarding the interpolating functions.

- The Hermite cubic and the second version of the rational cubic interpolant appear to be the most useful interpolation formulas. The first version of the rational cubic interpolant is consistently inferior to the second.
- The Bernstein quadratic interpolant is generally of comparable accuracy to the rational form mentioned above. We found it to be somewhat more difficult to program for the various special cases, which results in a corresponding increase in the complexity of computer code and execution time.
- The rational quadratic interpolant is of comparable accuracy to the SCM limited Hermite cubic for monotonic data, but it does not allow the flexibility of the Hermite cubic near extrema, or allow for the concave/convex structure provided by versions of the rational cubic interpolant. For data which have an extremum, this scheme is not recommended, because there is no alternative to assuming the slope goes to zero at a discrete extremum. This results in much larger errors in the vicinity of the extremum, than the cubic, rational cubic and piecewise quadratic spline forms.

Conclusions regarding the derivative estimates are:

- The geometric mean, harmonic mean and Fritsch-Butland derivative estimates are consistently less accurate than the others. Their virtue is their simplicity. While they may result in visually pleasing interpolants they are generally of insufficient accuracy for many applications. The rational-linear derivative estimate, equivalent to the derivative estimate suggested by McAllister and Roulier (1981), and the harmonic mean estimate suggested by Fritsch and Butland (1984) for equally spaced data, is the least accurate of all the slope estimates. The Fritsch-Butland slope is always more accurate than the rational linear slope.
- The Akima approximation performs extremely well for data with small-scale features, but less well for the broader, more rounded shapes. Careful examination of the results suggests the Akima scheme is actually quite accurate in the vicinity of the extrema, and much less accurate over the rest of the domain.
- Except for the intersection of straight lines such as triangular peaks where the Akima estimate shines, the Hyman derivative estimate is the most accurate, followed generally by the cubic, then arithmetic. The disadvantage of the cubic derivative approximation is that it does not provide for a continuous interpolant while the others do.
- Monotonicity constraints generally improve the interpolation of monotonic data and of data approaching a flat plateau. These constraints degrade the interpolation near extrema by not allowing any overshoot that might be implied in the underlying data. The derivative estimate is constrained to be zero in the vicinity of extrema with the C^1 form. The C^0 continuity constraint is less serious in this regard than the C^1.
- Where strict monotonicity is not required, relaxation of the monoticity condition at any extremum seems desirable to allow the interpolant to form an extremum somewhere other than at a data point. Application of Hyman's limiter for the Hermite cubic or the convexity condition for the rational cubic seems desirable to prevent overshooting in the approach to a flat or nearly flat plateau.

3. *ONE-DIMENSIONAL SEMI-LAGRANGIAN ADVECTION*

Based on the evaluation of the various shape-preserving interpolators described in the previous section, we chose those which rated well for further tests in one-dimensional semi-Lagrangian advection by a uniform wind field. The Eulerian form of the evolution equation for the advection by a constant wind field of a scalar field in the absence of sources and sinks is

$$\frac{\partial f(x,t)}{\partial t} + v\frac{\partial f(x,t)}{\partial x} = 0 \tag{3.1}$$

where f is a scalar field such as mixing ratio, t is time and v is the constant advection velocity. Given f at time t, the solution at time $t + \Delta t$ is

$$f(x, t + \Delta t) = f(\hat{x}, t) \tag{3.2}$$

where

$$\hat{x} = x - v\Delta t\,. \tag{3.3}$$

The evaluation in this section focuses exclusively on the interpolation aspect of the solution. Given the departure point $\hat{x}$, an interpolation is made to find $f(\hat{x}, t)$. The interpolated value is then the forecast value $f(x, t + \Delta t)$. We consider only the Hermite cubic and second version of the rational cubic interpolant coupled with arithmetic, cubic, Hyman and Akima derivative approximations. Unmodified and appropriately limited derivative estimates are considered.

We integrate the advection equation with $v\Delta t/\Delta x$ equal to $\pi/12$. We chose an irrational number so that the relative position of the test field and grid would change with time and given a long enough integration would become almost uniformly distributed over the domain. The equation was integrated for 1000 time steps with the solution plotted every 200. The plots are superimposed using a coordinate system that moves with the advecting velocity. The test shapes deform due to errors in the interpolation. The line code in the figures is such that the shorter the pattern members, the later in time the solution.

Rasch and Williamson (1987) present results from cosine bell and square wave initial conditions, with ten nonzero gridpoints. We select a few examples of the square wave tests to illustrate here the general properties observed. The figures show results from arithmetic, cubic, Hyman and Akima derivative estimates ordered top to bottom.

Figure 1 shows results from the Hermite cubic interpolant. The left column shows the unlimited forms of the derivative approximations. Strong oscillations greater than 10% of the true signal are evident with the Hyman and arithmetic derivative estimate. The cubic derivative estimate shows less over/undershoot and the Akima estimate the least. The Akima version seems to be evolving toward a peaked shape. Figure 1 (center column) shows results from the Hermite cubic interpolant when the derivative estimates are modified to satisfy the SCM0. The monotonicity condition has improved the solution by eliminating the overshoot at the expense of increased diffusion and a decrease in the maximum value, at least for the arithmetic and cubic derivatiave estimates. The Hyman

and Akima derivative versions are improved by the limiting procedure, with little or no increase in diffusion of the shape. Imposition of the SCM1 constraints (right column) results in a very substantial increase in the phase error of all versions except the cubic derivative estimate. However, this interpolator is C^1 only where the derivative estimates were modified.

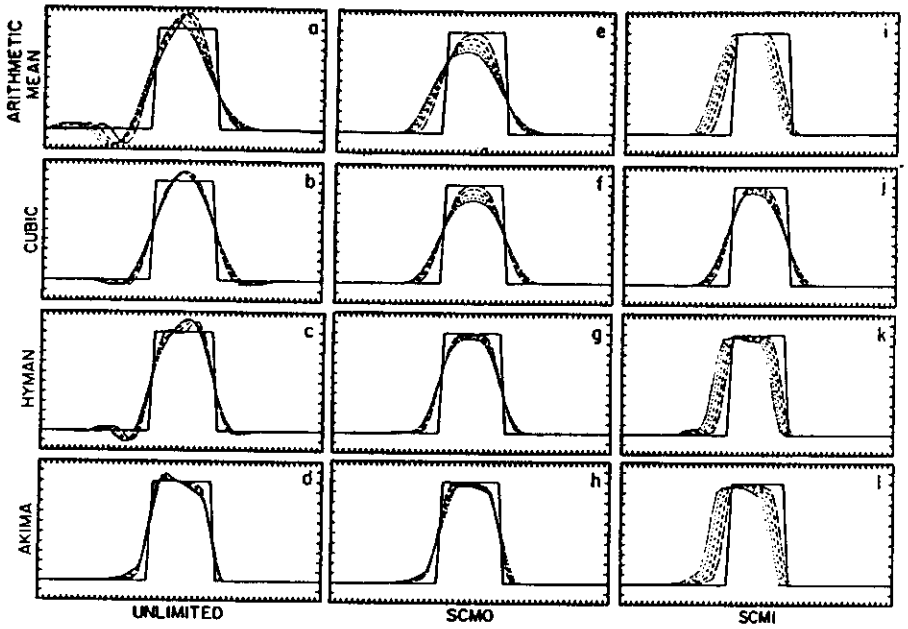

Fig. 1. Semi-Lagrangian advection with Hermite cubic interpolation of an initial square wave shown every 200 time steps (superimposed using a coordinate system that moves with the advecting velocity). The line code is such that the shorter the pattern members, the later in time the solution (the shortest pattern occasionally bleeds into an apparent solid line). Left column is for unlimited derivative estimates, center for estimates modified to satisfy SCM0 and right for SCM1. Top row for arthmetic mean derivative estimate, second row for cubic, third for Hyman and bottom for Akima.

The rational cubic interpolant (Fig. 2) results in a more rounded profile for the unlimited derivative estimates (left column) but provides a substantial reduction in the over/undershooting and dispersion when compared to the Hermite form (Fig. 1, left column) for the arithmetic, cubic and Hyman derivative estimates. Thus we consider this solution to be better. On the other hand, the solution using the Akima derivative estimate is worse with the rational than with the Hermite cubic interpolant. The C^1 necessary condition for monotonicity (Fig. 2, right column) increases the diffusion of the interpolation with the polynomial derivative estimates but leaves that with the Akima

Note that the C^1 monotonic rational interpolant does not show the increase in phase error seen with the C^1 Hermite monotonic interpolant in Fig. 1, right column.

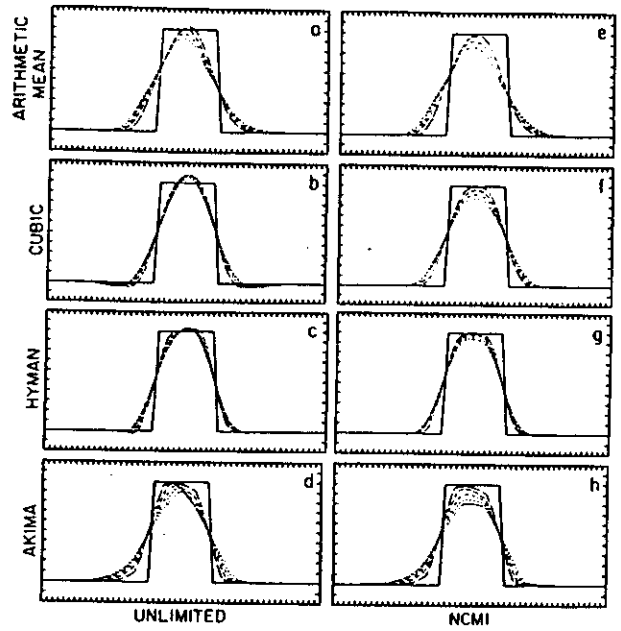

Fig. 2. As in Fig. 1 except with rational cubic interpolation. Left column is for unlimited derivative estimates and right for estimates modified to satisfy NCM1.

4. *TWO-DIMENSIONAL SEMI-LAGRANGIAN ADVECTION IN A PLANE*

We have also evaluated the Hermite and rational cubic interpolants for advection in two-dimensional Cartesian geometry. We consider three methods of applying shape preserving interpolation to the two-dimensional semi-Lagrangian advection problem. The first is to split the two-dimensional advection operator into two one-dimensinal operators via explicit fractional time steps or time-splitting. This approach was used by Purnell (1976) following Strang (1968) to obtain a scheme which was second order in time. Each fractional time step involves one-dimensional interpolation only.

The second method involves monotone piecewise bicubic interpolation. Carlson and Fritsch (1985) have extended their univariate piecewise cubic interpolation (Fritsch and

$$-\dot{\eta}\frac{\partial q}{\partial \eta} \rightarrow -\frac{1}{2\Delta\eta}\left[\dot{\eta}_{k+1/2}(q_{k+1}-q_k) + \dot{\eta}_{k-1/2}(q_k - q_{k-1})\right]$$

$\dot{\eta} < 0$, "neighbor borrowing" or flux control.

ere full values of indices refer to layers and half-values to interface: s the scheme used in the model, with the addition of a check for negat at the "fluxes" in the brackets of (1) would be altered to the extent nee ecific humidity (q) positive and at the same time the vertical sum of f remaining undesirable feature of (1), however, is the possibility of a f e maxima of q during the advection process. For example, if locally in a downward step in the distribution of moisture existed as sketched

Arakawa

"CICK"

"convective instability of computational kind"

$0 > \dot{\eta} \rightarrow$, const.

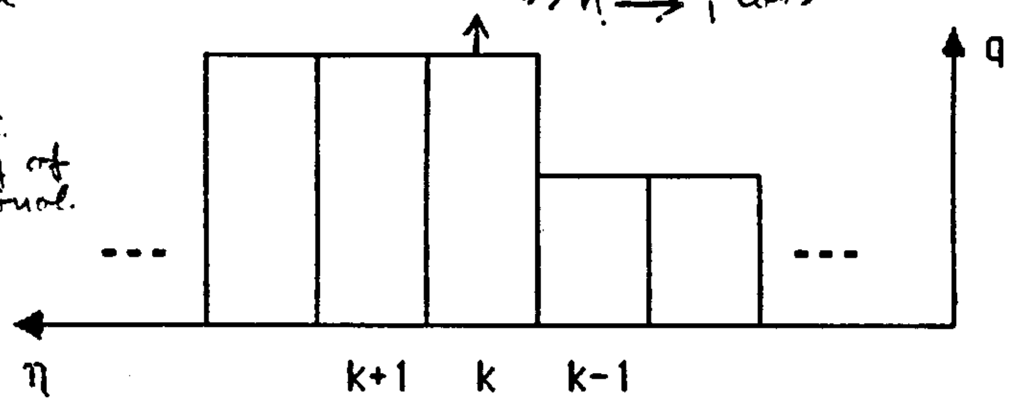

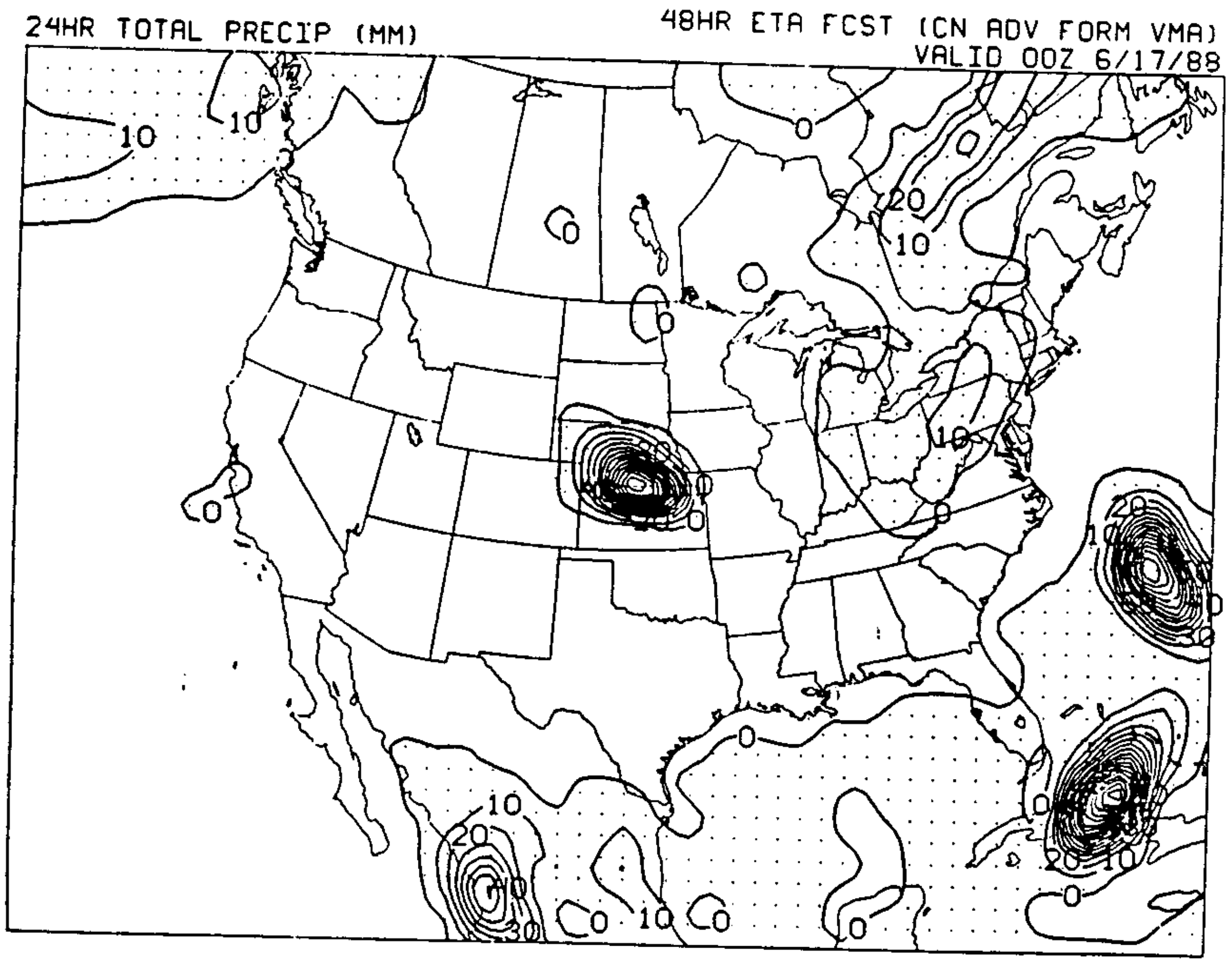

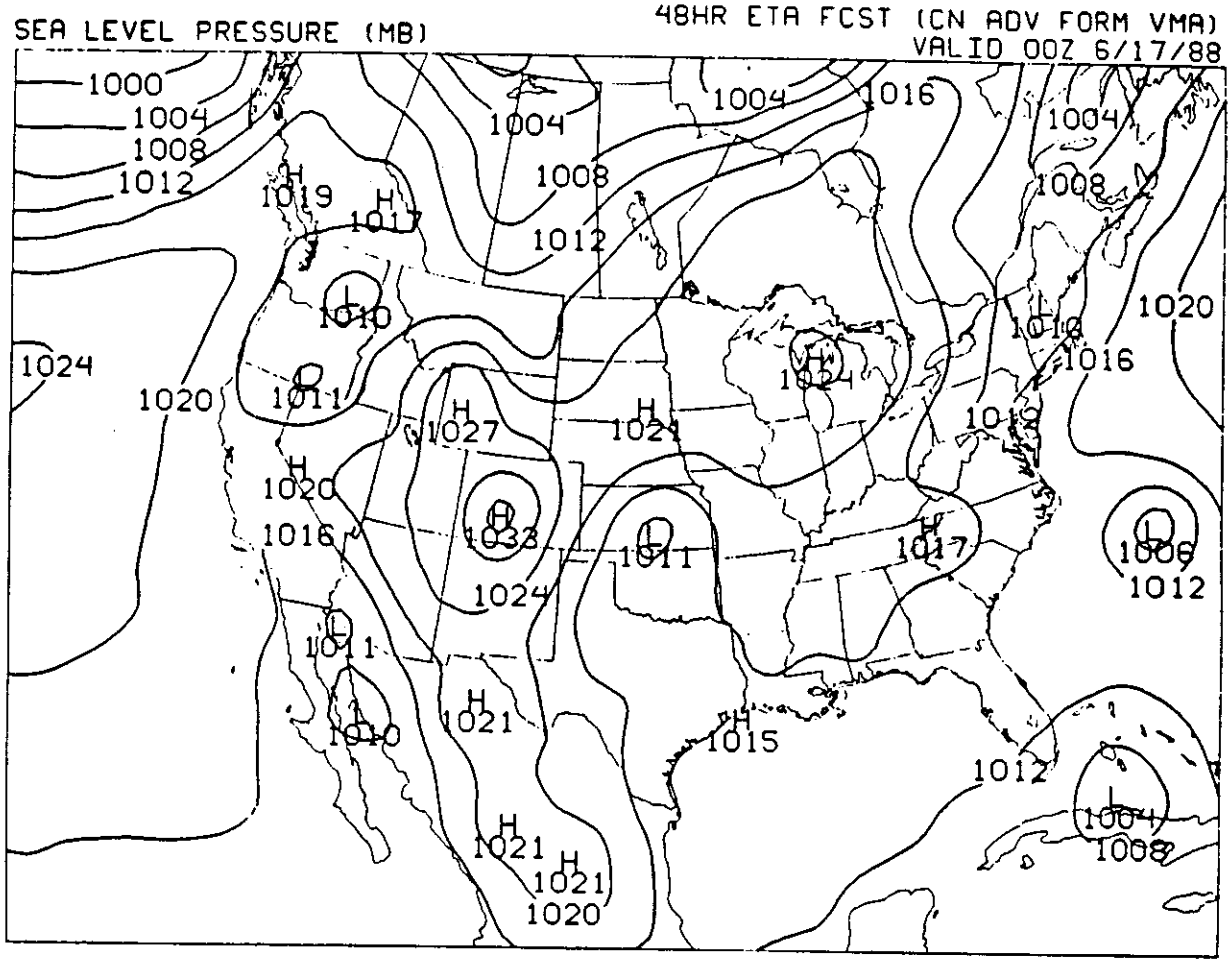
SEA LEVEL PRESSURE (MB)
48HR ETA FCST (CN ADV FORM VMA)
VALID 00Z 6/17/88
1000
1004
1008
1012
1016
1020
1024
1019
1017
1010
1011
1027
1021
1033
1015
1006
1012
1004
1008

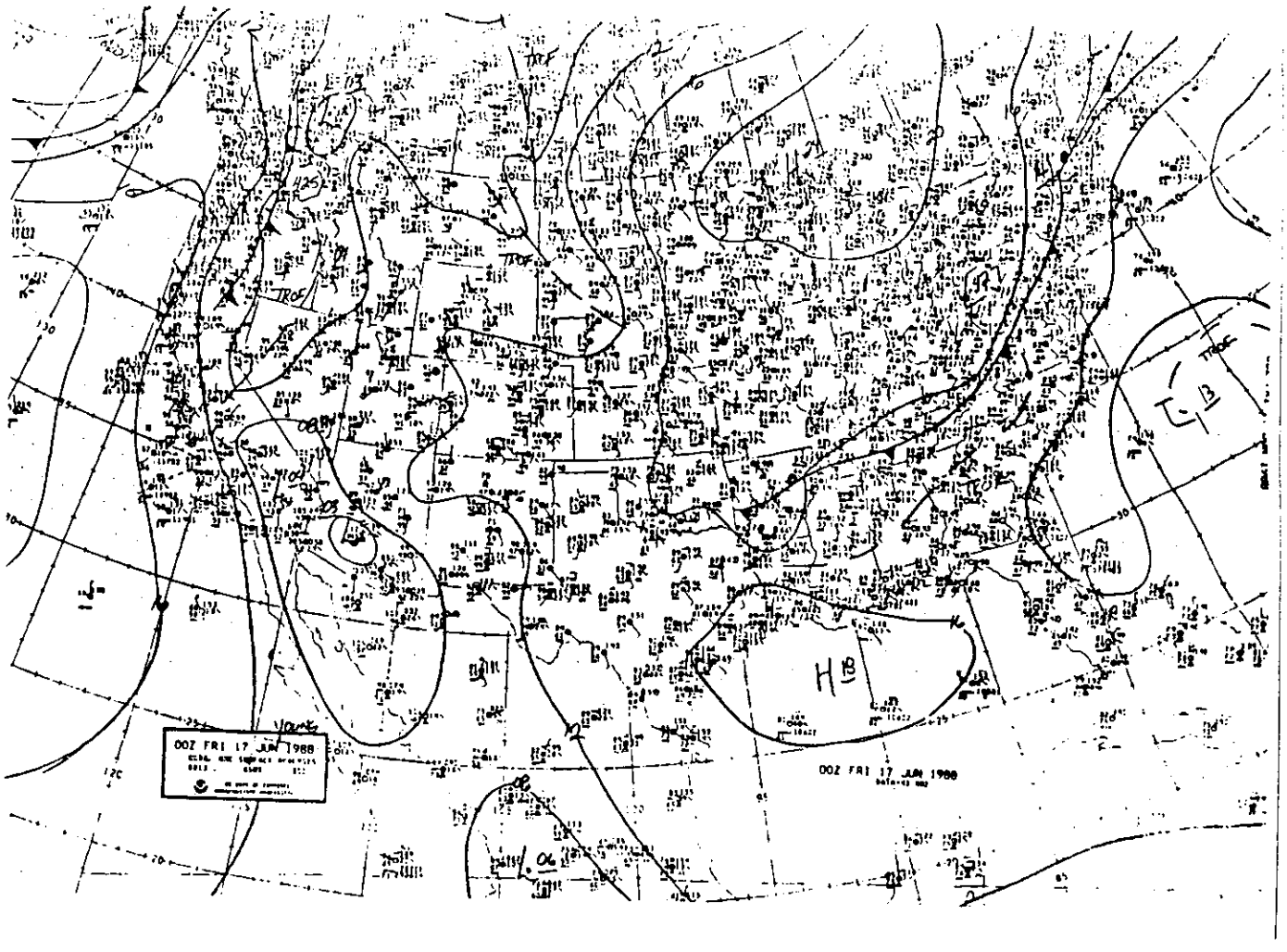
00Z FRI 17 JUN 1988
00Z FRI 17 JUN 1988

Godunov-type schemes:

Features (strengths) of the method:

- A "volume" (=grid box) scheme: grid point value is treated as a volume ("zone") average;
- Volume boundaries are treated as (possible) discontinuities, and physical properties of the fluid are used to calculate the interaction of neighboring fluid elements (zones)

Godunov (1959): introduced the method exploiting the solution to the so called Riemann's problem: two constant states in a tube, separated by a discontinuity. "Piecewise constant" method.

* Van Leer (1979): "piecewise linear" method.

Colella, Woodward (1984) "piecewise parabolic" method. (PPM)

Resulting schemes are not based on series expansions, and for accuracy they do not rely on smoothness of the fields !

$$\left(\frac{\partial \alpha}{\partial x} \rightarrow \frac{\alpha(x+\Delta x)-\alpha(x)}{\Delta x} \right.$$

is never done !)

* Lagrangian advection of boundaries

* Eulerian remap

- constant layer averages
  (piecewise constant, reduces to upstream scheme for constant velocity)
- slope adjustment
  piecewise linear (Van Leer 1977)
  piecewise parabolic (PPM) (Colella & Woodward 1984)

Step 3. Starting from the approximate initial values (3), integrate Eq. (1) over a nite time-step Δt. This is achieved by shifting the distribution $w(t^0, x)$ over a distance $\Delta t = a\,\Delta x$ along the x-axis:

$$W(t^1, x) = w(t^0, x - a\,\Delta x). \tag{4}$$

n view of the probable application of the scheme to systems of equations it is practical although not necessary) to restrict a by the usual Courant–Friedrichs–Lewy (CFL) ondition

$$|a| \leqslant 1. \tag{5}$$

Thus, the shift will never be greater than Δx.

Step 4 (*Step* 1). Determine the new mesh averages

$$\bar{w}^{i+(1/2)} = \frac{1}{\Delta x}\int_{x_i}^{x_{i+1}} W(t^1, x)\,dx. \tag{6}$$

These steps are illustrated in Fig. 1.

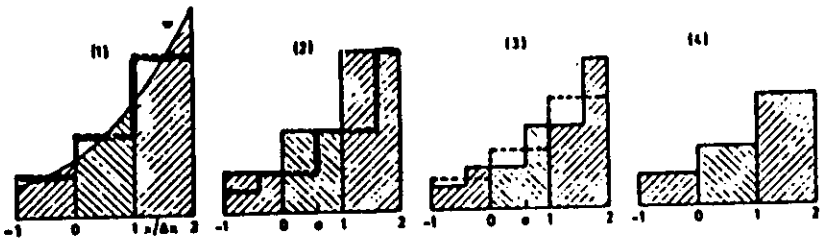

FIG. 1. The first-order upstream-centered scheme. (1) Determining the mesh averages (broken line) of the initial-value distribution (solid line). (2) The approximate initial-value distribution before (solid) and after (broken) convection over a distance $a\Delta x$. (3) Determining the new mesh averages (broken) of the convected distribution (solid). (4) The initial values for the next time step.

The numerical outcome of the above procedure is

$$\bar{w}^{1/2} = \begin{cases} (1 - |a|)\,\bar{w}_{1/2} + |a|\,\bar{w}_{-1/2} = \bar{w}_{1/2} - a\Delta_x\bar{w} & \text{if } a \geqslant 0, \\ (1 - |a|)\,\bar{w}_{1/2} + |a|\,\bar{w}_{3/2} = \bar{w}_{1/2} - a\Delta_x\bar{w} & \text{if } a < 0. \end{cases} \tag{7}$$

This is precisely the upstream-centered scheme of Courant, Isaacson, and Rees (CIR) [4] applied to mesh averages of w instead of nodal-point values (cf. Van Leer [1, Eq. (10)]).

Scheme (7) can also be related to the integral version of Eq. (1) in one space-time mesh, that is, to

$$\int_{x_0}^{x_1} w(t, x)\,dx\Big|_{t_0}^{t^1} + \int_{t_0}^{t^1} aw(t, x)\,dt\Big|_{x_0}^{x_1} = 0. \tag{8}$$

This equation is equivalent to

$$(\bar{w}^{1/2} - \bar{w}_{1/2})\,\Delta x + (\langle aw_1\rangle - \langle aw_0\rangle)\,\Delta t = 0, \tag{9}$$

where the angled brackets denote averaging over the time step. Equation (9) i tant in formulating the scheme for conservation laws (cf. Section 6). With tl wise constant initial values (3) we get

$$\langle aw_i\rangle = \begin{cases} a\bar{w}_{i-(1/2)} & \text{if } a \geqslant 0, \\ a\bar{w}_{i+(1/2)} & \text{if } a < 0, \end{cases}$$

and the familiar form (7) results. Note that, while Eq. (9) is exact, scheme (7 first-order accurate since the time averages $\langle aw_i\rangle$ are derived from the crudest approximation of the true initial-value distribution.

Once we recognize this, extension of the scheme towards a higher order of a becomes a straightforward matter. All we have to do is replace the true initi distribution $W(t^0, x)$ by a piecewise approximation that has a higher order of a than (3). In view of Eq. (2), where the mesh average of W is defined with resp constant weight function, it seems natural to further approximate W piec terms of Legendre polynomials:

$$w(t^0, x) = \bar{w}_{i+(1/2)} + (b_1)_{i+(1/2)}\frac{x - x_{i+(1/2)}}{\frac{1}{2}\Delta x} + (b_2)_{i+(1/2)}\left\{\left(\frac{x - x_{i+(1/2)}}{\frac{1}{2}\Delta x}\right)^2 - \frac{1}{3}\right\}$$

$$x_i < x < x_{i+1}$$

This ensures that integrating $w(t^0, x)$ with constant weight over any mesh (yields the proper average $\bar{w}_{i+(1/2)}$.

Let us first consider the possibilities of fitting the initial data in each me linear function. We may write

$$w(t^0, x) = \bar{w}_{i+(1/2)} + \frac{\bar{\Delta}_{i+(1/2)}w}{\Delta x}(x - x_{i+(1/2)}), \qquad x_i < x < x_{i+1},$$

where

$$\frac{\bar{\Delta}_{i+(1/2)}w}{\Delta x} \text{ is } \overline{\left(\frac{\partial w}{\partial x}\right)}_{i+(1/2)}$$

is some average of the gradient of $W(t^0, x)$ in the mesh (x_i, x_{i+1}). The evalua this average gradient belongs to Step 1; what sort of average is taken will be le for the moment. Equation (12) replaces Eq. (3) in Step 2; Step 3 remains the sar new procedure is illustrated in Fig. 2. Note that $w(t^0, x)$, although smoother Eq. (3), is still discontinuous. The scheme now updates $\bar{w}$ with second-order ac for $a \geqslant 0$ we get

$$\bar{w}^{1/2} = \bar{w}_{1/2} - a\Delta_x\bar{w} - (a/2)(1 - a)(\bar{\Delta}_{1/2}w - \bar{\Delta}_{-1/2}w).$$

This, again, is an upstream scheme; a central-difference scheme such as th Wendroff [5] scheme could never result from the procedure followed above respect to the integral equation (9) we have, for $a \geqslant 0$,

$$\langle aw_i\rangle = a\{\bar{w}_{i-(1/2)} + \tfrac{1}{2}(1 - a)\,\bar{\Delta}_{i-(1/2)}w\}.$$

The scheme is applied in the eta model in the following manner. As the first step of the slope adjustment procedure maxima and minima in the profile of q are identified. Slopes in these layers are not changed. For efficient vectorization slopes in the remaining layers are adjusted in an iterative procedure. With average values within layers kept constant in each sweep end points of the linear segments of the q profile across these layers which are at the side of the smaller of the two steps at its interfaces are moved to the mid-points of that step. This is illustrated in Fig. 4.4. The dotted line in the figure represents a hypothetical profile of q prior to the adjustment procedure. As the first step of this procedure values at layers k and k+3 would be identified as a minimum and as a maximum, respectively, and flagged not to be changed. Slopes which layers k+1 and k+2 would obtain as a result of the first sweep of the slope adjustment are shown by the two full lines in the figure. The code is at present set to have three iterations performed since inspection has shown that after three iterations little in view of adjustable steps remains and that computer time demands of three iterations are modest.

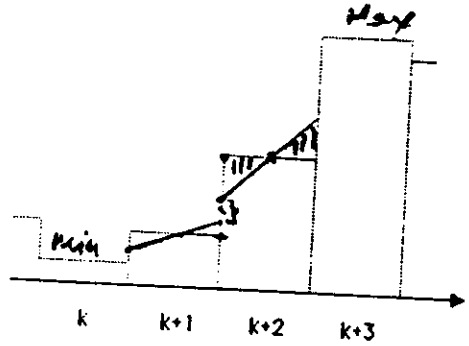

Fig. 4.4. Schematic illustration of the slope adjustment procedure of the eta model moisture advection scheme. The dotted line shows the original histogram of q. The full lines show the distribution of q in layers k+1 and k+2 following the first sweep of the adjustment code.

The [illegible] are in fact Eulerian advection problem versions of a [illegible] class of schemes referred to as Godunov-type schemes, or characteristic based schemes. They have been developed with the objective of simulating flows which contain discontinuities, such as shock waves. Most of this work has been done in the fields of aerodynamics and astrophysics, and applications to problems in meteorology are so far few and very recent